0022-202X/84/8303-0169$02.00/0
THE JOURNAL OF INVESTIGATIVE DERMATOLOGY, 83:169–174, 1984

Vol. 83, No. 3
Printed in U.S.A.

Characterization and Histogenesis of Tumors in the Hairless Mouse Produced by Low-Dosage Incremental Ultraviolet Radiation

C. H. GALLAGHER, D.V.Sc., PH.D., F.R.C.PATH., F.A.C.V.Sc., P. J. CANFIELD, B.V.Sc., PH.D., M.A.C.V.Sc., G. E. GREENOAK, AND VIVIENNE E. REEVE, B.Sc., PH.D.

Department of Veterinary Pathology, University of Sydney, New South Wales, Australia

Tumors were induced in the HRA/Skh-1 hairless mouse by repeated irradiations of minimally erythemal and suberythemal doses of UV radiation. Aspects of tumor induction were recorded using a combined system of mapping and gross descriptive classification. Tumors of epithelial and dermal (mesenchymal) origin were confirmed histologically and their types correlated well with those reported by earlier investigators. Among those classified, however, appendage tumors and hemangiomas have rarely been described.

The progression to malignancy of epithelial tumors was systematically characterized and was a consistent histogenic feature in our experiments. Squamous cell carcinomas represented a final stage for development arising ab initio or from other forms, in particular papillomas which commonly passed through intermediate forms toward definite malignancy.

While confirming previous studies of UV-induced tumors, this report extends our knowledge of their dynamics as this bears upon any experimental objective which includes an assessment of tumorigenicity.

Investigations into UV-induced tumorigenesis have commonly involved the use of constant doses of erythemal UV radiation [1–4]. However, in 1981, Willis, Menter, and Whyte [5] reported a method for rapidly inducing squamous cell carcinoma in the HRA/Skh-1 hairless mouse using exposures of highly erythemogenic but minimally injurious broad-spectrum UV radiation increased by 20% every 6th day. In these studies tumor counts have provided the main basis for interpreting the relative effectiveness of drugs and doses but reference to tumor types and their histogenesis has been made by some authors [4]. In our preliminary experiments on UV radiation-induced tumorigenesis, we used a similar method to Willis et al [5] and employed increasing weekly doses of both suberythemal (no visible effect) and minimal erythemal (mild reddening) UV irradiation. Not only the numbers of tumors but also their types and any progression or regression were noted for each regimen by a developed system of data recording. Comparisons were made, with a view to assessing the effectiveness of our irradiation systems, with tumor data presented by authors using constant doses of erythemal UV radiation and with those suspected sunlight-associated tumors occurring in humans.

This report presents information on our preliminary experiments. It provides a system for recording important tumor data and concentrates on the characterization of tumor types and their histogenesis, drawing attention to this as a parameter for the assessment of tumorigenicity.

Manuscript received June 28, 1983; accepted for publication March 23, 1984.

This work was supported by a Sydney University Cancer Research Grant.

Reprint requests to: Dr. C. H. Gallagher, Department of Veterinary Pathology, University of Sydney, N.S.W., Australia 2006.

MATERIALS AND METHODS

Animals

Hairless albino mice were chosen for their known susceptibility to UV tumor induction. For the first experiment a breeding nucleus of partially inbred HRA/Skh-1 mice was obtained from the Skin and Cancer Hospital, Temple University, Philadelphia, Pennsylvania to establish the first colony in Australia. For the second experiment fully inbred mice of the above strain were used. The mice were fed standard mouse pellets (Allied Feeds) and water ad lib. They were housed at 22°–25°C beneath automated 12 h of gold-light (GEC F40G0 No UV) and 12 h of dark.

Normal epidermis of the HRA/Skh-1 mouse is of a thickness comparable with human epidermis of the temple region, and is comprised of 3 to 4 cell layers without distinction into basal and spiny cell layers and a thin stratum granulosum and stratum corneum. After complete loss of the juvenile hair coat by 30 days from birth, the deep dermis is conspicuously altered by the presence of degenerating hair follicles with occasional inclusions of keratinous material. The incidence of spontaneous skin tumors was zero for the first experiment and was 1 in 1000 mice for the second.

Using precision vernier calipers, the skin thickness measurement of a pinch of dorsal skin of some hundreds of animals of increasing age showed that the whole skin is still growing in animals 6–8 weeks old, and in some animals 8–12 weeks of age, reaching a constant thickness in all animals after this time.

Groups of 11 females aged 8–12 weeks (1st experiment) and 20–28 weeks (2nd experiment) were maintained on vermiculite bedding in wire-topped plastic boxes 28 × 45 cm, for the duration of the experiments. With the wire cagetops removed, 4 boxes containing up to 12 unrestrained mice each could be irradiated simultaneously.

UV Irradiation

Radiation source: The 2 radiation sources used in this study were chosen as the first of a series designed to approach the sunlight spectrum.

For the 1st experiment, 2 120 fluorescent tubes (T2), one UVB (Oliphant FL40SE) and one UVA (Sylvania F40BL), were housed in a double batten with reflector. The radiation source used for the 2nd experiment differed by the addition of a further 2 UVA tubes (T4). The tubes were allowed to warm up for 5 min before exposures were started. Radiation intensity was measured at 297, 313, and 320–380 nm using International Light radiometers IL500A, IL530A, and IL442A with the appropriate detectors, diffusers, and filters. The flux is given in Table I. In addition, the spectral irradiance was measured between 250–400 nm, using a computer-controlled McPherson grating-monochromator with a prism disperser. A calibrated tungsten-halogen lamp was used as the reference source. The relative spectra, together with the solar spectral irradiance, obtained from the data of Habu, Suzuki, and Nagasuka (1981) and Kostowski et al (1980) [6] are normalized at 350 nm for comparative purposes (Fig 1).

Dosage regimens: Dosage regimens were selected on the basis of their ability to produce tumors with minimal or no observable skin changes before tumor appearance. Mice at 38 cm from the radiation source were exposed 5 days a week to 1 of 2 UV radiation dosages, determined from a graded series of exposures on untreated mice: first, an erythemal dose that induced a just visible reddening 4 h post UV irradiation and lasting for at least 24 h without desquamation; second, a suberythemal dose that did not induce any gross visible effect. Microscopically, a single minimal erythemal dose produced vascular dilatation and edema at 24 h which declined by 48 h. The epidermis first showed organization of the stratum germinativum into the characteristic "picket fence" ar-

TABLE I. *Emission intensities of the two UV radiation sources compared with Sydney summer sunlight at noon on 9.2.83, and experimental UV radiation dosages*

Radiation source	Wavelength (nm)	Flux (mW/cm^2)	Dosage mJ/cm^2			
			Suberythemal		Erythemal	
			Initial	Total	Initial	Total
T2	297	.015	1.8	121	5.4	362
Exp 1	313	.23	27.6	1,849	82.8	5,548
	320–380	.69	82.8	5,548	248.4	16,643
T4	297	.015	1.8	121	5.4	362
Exp 2	313	.227	27.2	1,825	81.7	5,475
	320–380	1.58	189.6	12,703	568.8	38,110
Sunlight	297	.004				
noon	313	.21				
9.2.83	320–380	2.30				

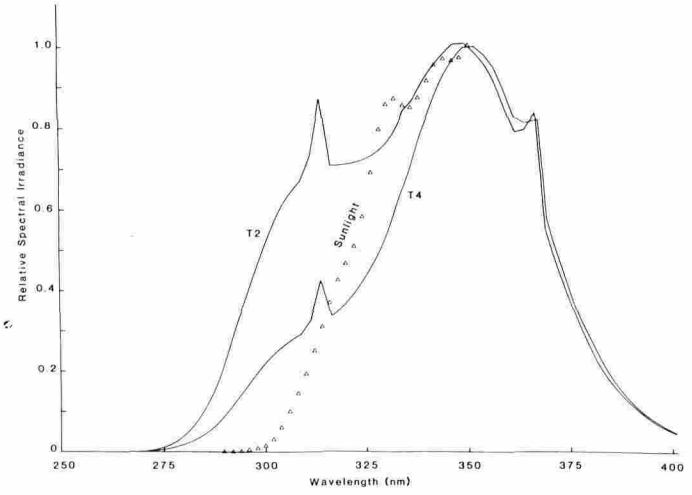

FIG 1. Relative spectral irradiance of the two artificial radiation sources, *T2* and *T4*, and *sunlight*, normalized at 350 nm.

rangement before active proliferation was noted at 48 and 72 h post irradiation. A single exposure to the suberythemal dosage induced only minimal changes: between 24–48 h a thickening of the epidermis was noticed but returned to normal by 72 h when a slightly increased keratin production was noted. Throughout the experiments the initial dose responses were maintained with no desquamation or burning noted in the incrementally increased erythemally dosed animals and no erythema appearing on those suberythemally dosed.

The initial doses of 2 min (suberythemal) and 6 min (minimum erythemal), respectively, were increased by 20% every week. The radiation intensity striking the dorsum was measured repeatedly at different positions of the irradiation area beneath the sources. To compensate for slight variations of intensity and for the small reduction in flux resulting from increased heat production and the aging of tubes, the boxes of mice were rotated during exposure and the entire treatment regimen reversed every week. With both radiation sources, 22 mice received 48 irradiations over 66 days of incrementally increased erythemal or suberythemal UV radiation and were observed for skin pathology and tumors until day 200 from the start.

Gross Examination and Light Microscopic Examination

All mice were distinguished from one another by a system of ear marking. The development and appearance of tumors were noted weekly on a chart in two ways. First, the site, size, and time of appearance or disappearance of each tumor was charted on a schematic representation of the mouse. Second, each tumor was described in terms of letters and numbers based on a classification (Table II) which allowed broad preliminary tumor typing that could be correlated later with histologic analysis. Over the course of the experiments, some tumors received several classifications due to progression or regression. Tumors for histologic examination were excised in their entirety, fixed in 10% phosphate-buffered formalin, and embedded in paraffin. Five to six micron sections were stained routinely with hematoxylin and eosin (H&E), and occasionally with periodic acid-Schiff reagent (PAS), toluidine blue, van Gieson's method for connective tissue, and Sweet's method for reticulin [7].

TABLE II. *Classification for gross appearance of tumors*

A.	*Macule*: A well-defined, discolored area
B.	*Papule*: A nondescript, raised epidermal mass less than 1 mm in diameter
B1	Red
B2	Ulcerated
C.	*Exophytic tumor*: Growth (> 1 mm) projecting from the surface of the skin
C1	Sessile base
C2	Pedunculated base
C3	Red
C4	Translucent
D.	*Endophytic tumor*: Inward growth (> 1 mm), particularly of the central area
D1	Well-defined, regular, raised borders
D2	Borders poorly defined, underrunning the surrounding epidermis
D3	Raised center
E.	*Unusual tumor (includes dermal tumors)*: Described in detail
X.	*Reddened dermal reaction around tumor*: Used in combination with other classifications

TABLE III. *Histologic classification of UV-induced tumors*

Epithelial in origin	Dermal in origin
Appendage cysts	Fibroma
Focal hyperplasia with or without distortion of epidermis	Hemangioma
Appendage/basal tumor	Fibrosarcoma
Papilloma	Undifferentiated sarcoma
Keratoacanthoma-like tumor	
Carcinoma in situ	
Squamous cell carcinoma	
Undifferentiated carcinoma	

A complete range of histologic sections of sunlight-associated human skin tumors, made available by the Skin and Cancer Foundation (St. Vincents Hospital, Darlinghurst, N.S.W.) was examined with a view to their comparability to experimentally UV-induced skin tumors in mice.

RESULTS

Regardless of the source, spectral differences and, irrespective of UV radiation dosage, the main types of tumors, their histogenesis, and the mode of progression were similar for both experiments. Consequently, these aspects of the two experiments are presented in a combined form.

Tumor Types

The types of tumors produced are presented in Table III. Tumors were classified according to their histologic similarity to skin tumors in humans. The term "tumor-like" has been used when some features vary from those present in comparable tumors in humans.

On gross appearance alone, at the end of the experiments, papillomas were by far the most common tumor. Papules, which represented a variety of histologic types, were next in frequency,

followed by endophytic tumors representing either keratoacanthoma-like lesions or squamous cell carcinomas. Macules (appendage tumors or areas of focal epidermal hyperplasia with or without distortion) were the least common of the epidermal changes, while dermal swellings were uncommon. Although the gross tumor appearance gave good indication of the histologic tumor types, it was apparent on examination that microscopic foci of progression were sometimes present. Table IV presents the main histologic tumor types for the two experiments and their frequency of occurrence.

Epithelial in origin: Appendage cysts and focal epidermal hyperplasia with or without distortion were common. The appendage cysts have been included in Table III, as grossly they can be mistaken for true tumors. Appendage cysts were predominantly pilar cysts, related to degenerate hair follicles, and they presented as white nodular lesions of varying size. In one instance a cyst was of true epidermal origin. Focal epidermal hyperplasia without distortion presented as macules while those with distinct distortion presented as papules or macules. They were considered to be either preneoplastic or early neoplastic proliferations but were classified as actinic keratoses as they had few similar features.

Appendage tumors were uncommon and presented as slow-growing discolored macules histologically consisting of numerous branching paired rows of cuboidal cells extending down from the epidermis near the pilosebaceous complexes (Figs 2, 3). Although these tumors resembled sweat gland tumors in humans, their histogenesis was not determined as mice are reported not to have apocrine glands while eccrine glands are restricted to the foot pads [8]. On two occasions macules consisted also of areas of sebaceous hyperplasia.

Papillomas were common, slow-growing, and were either sessile-based on pedunculated (Figs 4, 5). Pedunculated papillomas, which were equal in frequency to sessile-based papillomas, were translucent when containing loose connective tissue and were red when containing many telangiectactic vessels, some with thrombi, in the stroma (Fig 6). In no case was the stroma associated with the pedunculated papillomas considered to be neoplastic, therefore the term fibropapilloma was not used. Some papillomas had 2–3 projections while others had many. Epidermal cell layers were well organized and had a prominent granular cell layer.

Tumors classified as carcinomas in situ were more common than endophytic tumors. They presented as papules sometimes slightly endophytic (Fig 7). They consisted of focal areas of hyperplastic epidermis, usually poorly organized into layers, which resembled sheets of undifferentiated epithelium (Fig 8). In some cases cell pleomorphism, characterized by bizarre nuclear forms and multinucleate cells (Fig 9), was obvious and resembled that present in Bowenoid actinic keratoses in humans. The basement membrane of the epidermis was intact.

Lesions resembling keratoacanthomas in humans were less frequent than squamous cell carcinoma. They presented as endophytic tumors, usually with a depressed central area and raised borders (Fig 10). Occasionally, the central area was raised due to excessive keratinization. Histologically, the epidermal proliferation was invaginating en masse into the dermis and, at times, had penetrated down to the level of the muscle (Figs 11, 12). The epidermal cells usually showed organization into layers but at times this was indistinct and cellular features resembled those present in carcinomas in situ (Fig 13). Unlike keratoacanthomas in humans, the borders were usually distinct and few clear, ballooned epidermal cells were present. A dermal inflammatory response, characterized by infiltrates of neutrophils and lymphocytes, was commonly present around the base of the tumor.

Squamous cell carcinomas presented grossly as 3 main forms. Occasionally they presented as papules with ulcerated centers which, at times, underran the surrounding epidermis. Others presented as endophytic tumors with verrucose centers but always with irregular outlines and a reddened base. Most presented as ulcerated endophytic tumors with irregular reddened bases (Fig 14). Histologically, most squamous cell carcinomas showed differentiation, either as keratin whorls or as individual cell keratinization. Invasion into the dermis was either by individual cells or by groups and evoked a strong inflammatory response (Figs 15, 16). Of two undifferentiated carcinomas, one was suspected of being a spindling squamous cell carcinoma on the basis of its site of origin while the other had an obscure histogenesis. Both undifferentiated carcinomas presented as rapidly growing ulcerated nodules.

Dermal (mesenchymal) in origin: Most dermal tumors presented as oval to spherical nodules covered by smooth epidermis. Most were hemangiomas with the other types rare. Hemangiomas tended to be markedly red and cystic. Histologically, they were usually cavernous and commonly distorted the lower layers of the epidermis. A fibroma was pink and opaque and consisted of active fibroblasts and fibrocytes, and substantial amounts of collagen. A fibrosarcoma grew rapidly and was large and irregularly reddened. It had minimal collagen formation and marked mitotic activity and nuclear pleomorphism. One undifferentiated sarcoma, diagnosed on the basis of a reticulin stain, had areas of both osteoid and vessel formation.

TABLE IV. *Histologic tumor types and their frequencies determined from total numbers, gross appearance, and microscopic examination of representative types*

	Experiment 1 (T2)	Experiment 2 (T4)
Total number of tumors	159	56
Papillomas	61.6[a] (98)[b]	53.6 (30)
Carcinoma in situ	19.5 (31)	21.4 (12)
Focal epidermal hyperplasia and distortion	4.4 (7)	7.1 (4)
Squamous cell carcinoma	8.2 (13)	9 (5)
Keratoacanthoma	2.5 (4)	1.8 (1)
Appendage tumor	0.6 (1)	1.8 (1)
Undifferentiated carcinoma	0.6 (1)	—
Dermal tumors	2.5 (4)	5.4 (3)

[a] Frequency in percentage.
[b] Number of tumors shown in parentheses.

Tumor progression/regression

During the course of the two experiments both papules and papillomas regressed. Papules tended to regress in the early stages while pedunculated and sessile-based papillomas tended to regress in the middle to end periods of the experiments. Regression was not noticed for endophytic tumors. In Exp 1 the regression rate was 25.7% (55/214 tumors) while in Exp 2 the regression rate was 28.2% (22/78 tumors).

Tumor progression was suspected at the gross level due to changes in basic tumor appearance and/or rate of growth. Confirmation was provided by histologic examination which also detected microscopic foci of progression in other tumors not varying on gross examination. In Exp 1 the progression rate was 21.4% (34/159 tumors) and in Exp 2 it was 17.8 (10/56 tumors).

Papules developed into exophytic (papillomas) and endophytic (keratoacanthomas, squamous cell carcinomas) tumors. Others remained as papules, usually presenting as carcinomas in situ. The time period before progression of papules was variable but on development of malignancy an increase in growth was usually noticed. Apart from the development of squamous cell carcinomas directly from papular carcinomas in situ, some developed from papillomas and keratoacanthoma-like tumors. The rate of growth of papillomas and keratoacanthomas was variable but usually less than on their progression to squamous cell carcinoma. Both sessile-based and pedunculated papillomas, at times, developed zones of epidermal disorganization and pleomorphism (Figs 17, 18) which progressed to invade the dermis and become squamous cell carcinomas.

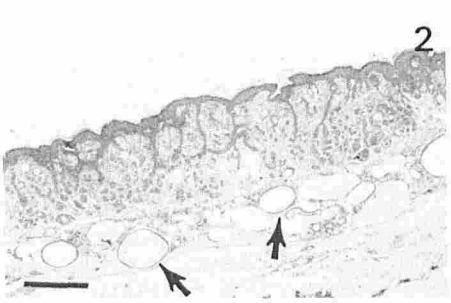

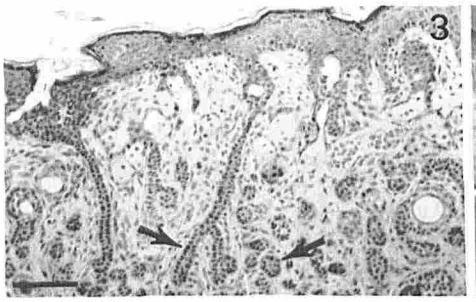

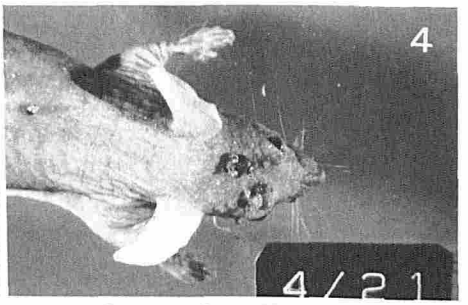

FIG 2. Appendage tumor, representing grossly as a macule. Also present are appendage cysts (*arrow*). H&E × 30. *Bar* = 330 μm.
FIG 3. Higher-power view of Fig 2 showing branching paired rows and circular accumulation of cuboidal cells (*arrows*). H&E × 100. *Bar* = 100 μm.
FIG 4. White to red papillomas, predominantly pedunculated. Head papillomas commonly occurred in clusters.

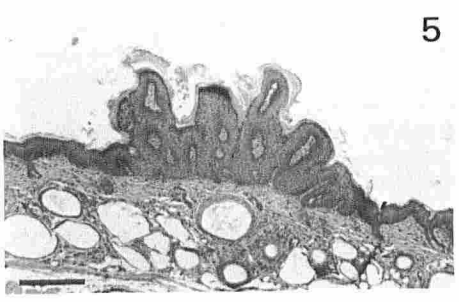

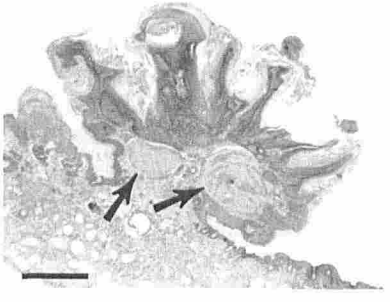

FIG 5. Beginning of a sessile-based papilloma. H&E × 30. *Bar* = 330 μm.
FIG 6. Pedunculated papilloma with large thrombi (*arrows*). H&E × 15. *Bar* = 660 μm.
FIG 7. Carcinoma in situ presenting as an endophytic papular proliferation of epidermis. H&E × 15. *Bar* = 660 μm.

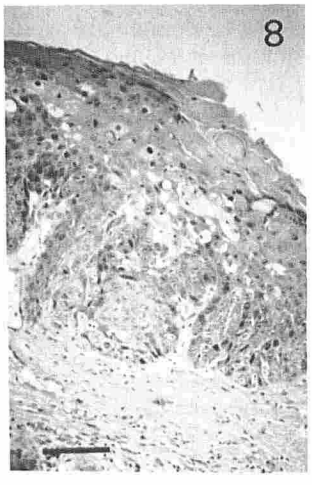

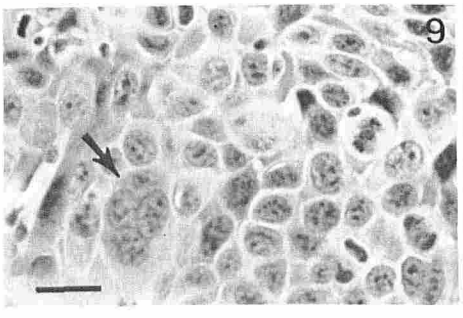

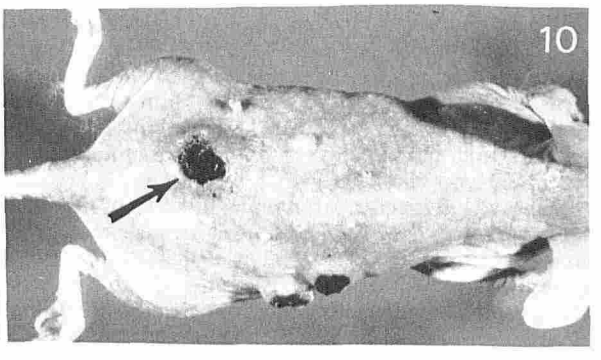

FIG 8. Carcinoma in situ showing sheets of cells and disorganized layering of epidermis. The granular cell layer is absent. H&E × 100. *Bar* = 100 μm.
FIG 9. Carcinoma in situ. Multinucleate cell (*arrow*) and cell pleomorphism. H&E × 400. *Bar* = 25 μm.
FIG 10. Three endophytic tumors are present. The two present on the lateral body wall were keratoacanthoma-like tumors. The one present on the dorsum (*arrow*) had early progression to a squamous cell carcinoma. Various papules and papillomas are present on the dorsum.

Keratoacanthoma-like tumors also developed transitional forms, with the epidermal cells losing differentiation and appearing rather like carcinomas in situ before invading the dermis. Squamous cell carcinomas appeared also to develop directly from non-neoplastic treated skin, with the well-differentiated ones growing at a slower rate than the less-differentiated squamous cell carcinomas.

At the gross level, progression to malignancy by epidermal tumors was usually accompanied by a reddening of the tissue around the tumor, or for keratoacanthomas, an intensification of the dermal inflammation. At times, especially for transitional forms and for the more rapidly growing, less-differentiated squamous cell carcinomas, the red zone was not distinct and dermal inflammation was detected only on microscopic examination.

DISCUSSION

A system has been devised allowing the objective assessment of all aspects of tumor production and thereby refining the mesh for our understanding of UV radiation carcinogenesis. While most workers have emphasized the significance of numbers of tumors produced within given experimental conditions and objectives, our results bear out and extend the suggestion made by Willis et al [5] that tumor types are also important. We suggest furthermore, that the proportion of their types and

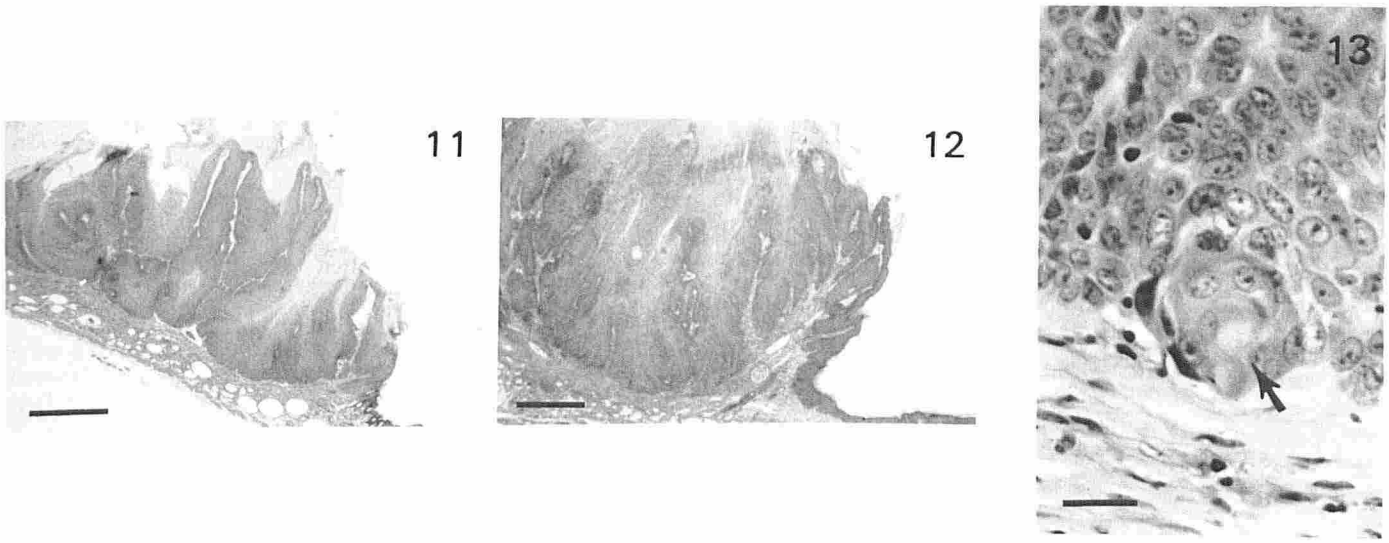

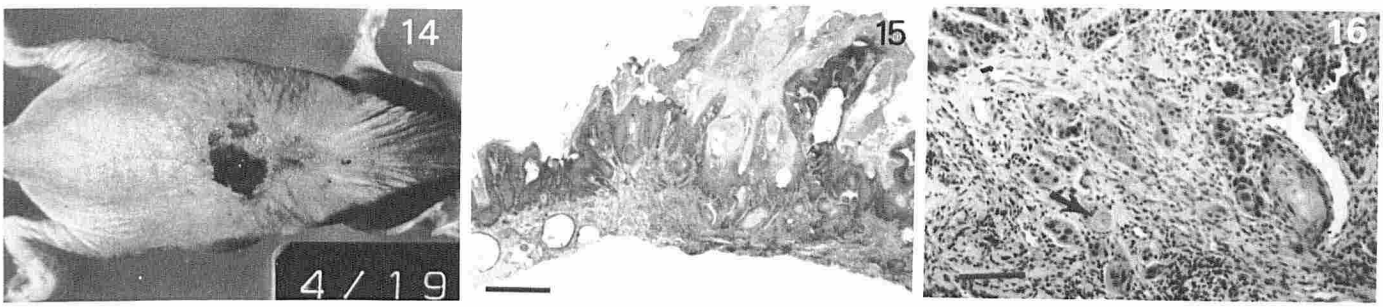

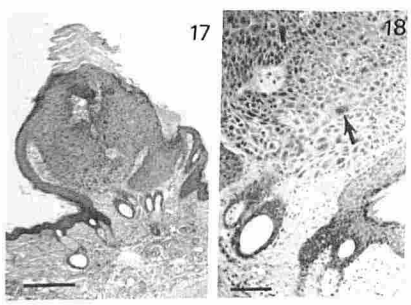

FIG 11. Early endophytic tumor resembling keratoacanthoma. H&E × 15. *Bar* = 660 μm.

FIG 12. More advanced keratoacanthoma-like lesion with the base extending down to the subcutis. H&E × 15. *Bar* = 660 μm.

FIG 13. Sheets of undifferentiated epithelium at the base of a keratoacanthoma-like lesion. A keratinizing nodule is present (*arrow*). H&E × 400. *Bar* = 25 μm.

FIG 14. Ulcerated squamous cell carcinoma on the dorsum.

FIG 15. Verrucose squamous cell carcinoma showing invasion of subcutis. H&E × 15. *Bar* = 660 μm.

FIG 16. Invasion of the dermis by clusters of squamous cells and individually keratinizing cells (*arrow*). H&E × 100. *Bar* = 100 μm.

FIG 17. Pedunculated papilloma. H&E × 30. *Bar* = 330 μm.

FIG 18. Base of papilloma in Fig 17 showing cellular pleomorphism and layer disorganization. Multinucleate cells are present (*arrow*). H&E × 100. *Bar* = 100 μm.

patterns of progression/regression are of equal importance. The consideration of these aspects of tumor induction in the two experiments with different radiation sources has shown a similarity of tumor types, underscored in both cases by a pattern of progression, hitherto unreported.

The types of UV-induced tumors produced in our experiments correlate well with those produced in studies using much higher and constant doses [3,4]. Moreover, both the minimally erythemal and suberythemal doses of UV radiation used in our experiments produced the same range of tumor types. Hemangiomas and appendage/basal cell tumors, however, were not noted by Kligman and Kligman [4], and Stenback [3] stated that vascular tumors have been found infrequently in irradiated mice and that appendage tumor formation is not as widespread in UV-treated animals as in chemical carcinogen-treated rats.

Epstein and Epstein [1], in earlier studies on UV-induced carcinogenesis, stated that squamous cell carcinoma can evolve from both benign hyperplasia and actinic keratosis-like changes. In 1981 Kligman and Kligman [4] commented specifically on the development of squamous cell carcinoma from sessile-based papillomas and keratoacanthomas. Tumor progression and regression was a consistent feature in our experiments and the data recording system allowed important observations of such histogenesis. Squamous cell carcinoma developed from papular carcinoma in situ, papillomas, and keratoacanthoma-like tumors. The latter type was so called after Strickland, Burns, and Albert [9] who noted large crateriform lesions lined by multilayered squamous epithelium which were produced exclusively of all other tumor types by UV irradiation of rats. These keratoacanthoma-like tumors, as the denotation suggests, are similar but not identical to keratoacanthomas found in human skin. Both pedunculated and sessile-based papillomas showed marked tendencies of progression to malignancy. This is in contrast to the findings of Kligman and Kligman [4] who stated that pedunculated papillomas, called by them fibropapillomas, are more typical of chemical carcinogenesis, and when induced by UV irradiation, generally remain benign. Histologically, transitional tumor types were frequently observed, to complicate classifications based on human skin tumor types. As Lever and Schaumburg-Lever [10] comment in regard to squamous cell carcinoma and solar keratoses in humans, their differences lay often in the degree rather than type of change. However, squamous cell carcinoma in our study was recorded only when obvious invasion of the dermis had occurred. In consideration of these aspects of progression we considered all epidermal tumors to be potentially malignant where malignancy itself may be used as an additional factor for the assessment of experimental results.

We thank Stephanie Sharkey and Suleyman Sari for care in the breeding, maintaining, and experimental handling of the mice; Beverley Horsburgh, Alan Kunovsky, and Vanda Bagnall for technical assistance in histology; Ian Weston for photographic assistance; and Graham Levitt and Rex Barry for electrical expertise. Dr. S. Kossard of the Skin and Cancer Foundation, St. Vincent's Hospital, Darlinghurst, N.S.W. assisted in aspects of comparative histologic diagnoses. Thanks also to Frank Wilkinson of the National Standards Laboratory, C.S.I.R.O. who performed the spectroradiometric analysis of the UV radiation sources. Ms. Sally Spence typed the manuscript.

REFERENCES

1. Epstein JH, Epstein WL: A study of tumor types produced by ultraviolet light in hairless and hairy mice. J Invest Dermatol 41:463–473, 1963
2. Winkelmann RK, Zollman PE, Baldes EJ: Squamous cell carcinoma produced by ultraviolet light in hairless mice. J Invest Dermatol 40:217–224, 1963
3. Stenback F: Life history and histopathology of ultraviolet light-induced skin tumors. Natl Cancer Inst Monograph 50:57–70, 1978
4. Kligman LH, Kligman AM: Histogenesis and progression of ultraviolet light-induced tumors in hairless mice. JNCI 67:1289–1297, 1981
5. Willis I, Menter JM, Whyte HJ: The rapid induction of cancers in the hairless mouse utilizing the principle of photoaugmentation. J Invest Dermatol 76:404–408, 1981
6. Habu M, Suzuki M, Nagasaka T: Measurement of the solar spectral irradiance at Tanaohi, Tokyo, (I), (II). Researches of the Electrotechnical Laboratory, Japan, Nos. 812, 813, 1981
7. Culling CFD: Handbook of Histopathological and Histochemical Techniques, 3d ed. London, Butterworths, 1975
8. Neilsen SW: Diseases of skin, Pathology of Laboratory Animals. Edited by Benirschke, Garner, Junes. New York, Springer-Verlag, 1978, p 581
9. Strickland PT, Burns FJ, Albert RE: Induction of skin tumours in the rat by single exposure to ultraviolet radiation. Photochem Photobiol 30:683–688, 1979
10. Lever FW, Schaumburg-Lever G: Tumors and cysts of the epidermis, Histopathology of the Skin, 5th ed. Philadelphia, JB Lippincott, 1975, chap 25